Fast centromeric repeat turnover provides a glimpse into satellite DNA evolution in *Nothobranchius* annual killifishes

Anna Voleníková[1,2], Karolína Lukšíková[1,3], Pablo Mora[2,4], Tomáš Pavlica[1,5], Marie Altmanová[1,6], Jana Štundlová[1,2,5], Šárka Pelikánová[1], Sergey A. Simanovsky[7], Marek Jankásek[1,5], Martin Reichard[8,9,10], Petr Nguyen[1,2¶*], Alexandr Sember[1¶*]

[1] Institute of Animal Physiology and Genetics, Czech Academy of Sciences, Liběchov, Czech Republic
[2] University of South Bohemia, Faculty of Science, České Budějovice, Czech Republic
[3] Department of Genetics and Microbiology, Faculty of Science, Charles University, Prague, Czech Republic
[4] Department of Experimental Biology, Genetics Area, University of Jaén, Jaén, Spain
[5] Department of Zoology, Faculty of Science, Charles University, Prague, Czech Republic
[6] Department of Ecology, Faculty of Science, Charles University, Prague, Czech Republic
[7] Severtsov Institute of Ecology and Evolution, Russian Academy of Sciences, Moscow, Russia
[8] Institute of Vertebrate Biology, Czech Academy of Sciences, Czech Republic
[9] Department of Ecology and Vertebrate Zoology, University of Łódź, Łódź, Poland
[10] Department of Botany and Zoology, Faculty of Science, Masaryk University, Brno, Czech Republic

[*] **Correspondence**: sember@iapg.cas.cz (AS); petr.nguyen@prf.jcu.cz (PN)

¶These authors contributed equally to this work.

ORCID IDs:
A.V.: 0000-0002-9504-8044
P.M.: 0000-0001-7967-3379
M.A.: 0000-0001-7193-8918
J.S.: 0000-0001-7890-1608
S.A.S: 0000-0002-0830-7977
M.J.: 0000-0002-1467-8790
M.R.: 0000-0002-9306-0074
P.N.: 0000-0003-1395-4287
A.S.: 0000-0003-4441-9615

Abstract

Satellite DNA (satDNA) is rapidly evolving class of tandem repeats with some motifs being involved in centromere organization and function. Rapid co-evolution of centromeric satDNA and associated proteins has been mostly attributed to the so-called centromere drive. To identify repeats associated with centromeric regions and test for the role of meiotic drive in their evolution, we investigated satDNA across Southern and Coastal clades of African annual killifishes of the genus *Nothobranchius*. C-banding showed expansion of (peri)centromeric heterochromatin regions in the Southern-clade killifishes. Molecular cytogenetic and bioinformatic analyses further revealed that two previously identified satellites, Nfu-SatA and Nfu-SatB, are associated with centromeres only in one lineage of the Southern clade. Nfu-SatB was, however, detected outside centromeres also in other members of the Coastal clade, which is consistent with the "library" hypothesis of satDNA evolution. We also identified a novel satDNA, Cl-36, associated with (peri)centromeres in *N. foerschi*, *N. guentheri* and *N. rubripinnis* from the Coastal clade. Our findings could be explained by centromere drive shaping karyotype change and centromeric repeat turnover in *Nothobranchius* species with possible reversal of spindle polarity within the Southern clade.

Keywords: centromere drive; constitutive heterochromatin; library hypothesis; RepeatExplorer; repetitive sequences; satDNA

1. Introduction

African killifishes from the genus *Nothobranchius* (Peters, 1868) (Aplocheiloidei: Nothobranchiidae) are small freshwater fishes with bigger and more colorful males compared to smaller and dull females (Wildekamp 2004; Berois et al. 2016). The genus is monophyletic and currently comprises over 90 species (Nagy and Watters 2021; Fricke et al. 2023) partitioned into seven evolutionary lineages (van der Merwe et al. 2021). *Nothobranchius* spp. are adapted to periodic droughts driven by cycles of rainy and dry seasons in south-eastern African savannahs, where they survive in isolated pools, temporarily flooded by rainwater (Blažek et al. 2013; Furness 2016; Cellerino et al. 2016). Having the shortest life cycle among vertebrates, the turquoise killifish *N. furzeri* (Jubb, 1971) became a popular model system for aging research (Cellerino et al. 2016; Hu and Brunet 2018). Besides, the unique biology of killifishes offers many advantages for studies related to developmental biology, population dynamics and evolution (Cellerino et al. 2016; Terzibasi Tozzini and Cellerino 2020). For instance, their mating system and sexual dimorphism make them attractive for studies of reproductive isolation and sexual selection (Berois et al. 2016; Cellerino et al. 2016).

Nothobranchius killifishes became of interest also to genome and sex chromosome research. Studies reported high repetitive DNA content in *Nothobranchius* genomes (Reichwald et al. 2009, 2015; Cui et al. 2019; Štundlová et al. 2022) and wide variation in diploid chromosome numbers (2n = 16–50) and karyotype structures in 73 studied representatives (Krysanov et al. 2016; Krysanov and Demidova 2018; Krysanov et al. 2023). Moreover, a multiple sex chromosome system of the X_1X_2Y type has been cytogenetically identified in six distant *Nothobranchius* spp., which suggests remarkable sex chromosome evolution (Ewulonu et al. 1985; Krysanov et al. 2016; Krysanov and Demidova 2018). Intriguingly, the *N. furzeri* genome sequence revealed an XY sex chromosome pair with polymorphic size of a non-recombining region in different populations (Reichwald et al. 2015; Willemsen et al. 2020). It was hypothesized that the *N. furzeri* Y chromosome polymorphism represents an early stage of sex chromosome evolution (Reichwald et al. 2015). However, physical mapping of various repeats in *N. furzeri* and its sister species *N. kadleci* revealed that repetitive DNA landscape differs considerably between their X and Y chromosomes and these differences extend beyond the non-recombining regions. One particular difference between the X and Y chromosomes was a largely reduced block of constitutive heterochromatin in the centromeric region on Y chromosomes in two out of three examined populations (Štundlová et al. 2022). This region overlapped with hybridization signals of fluorescence *in situ* hybridization (FISH) with two

96 repeats associated with *N. furzeri* centromeres, the Nfu-SatA and Nfu-SatB (Reichwald et al.
97 2009; Štundlová et al. 2022).

98 Certain satellite DNAs (satDNA), i.e. tandemly repeated DNA class with rapid molecular
99 evolution (Plohl et al. 2012; Garrido-Ramos 2017; Thakur et al. 2021), can be associated with
100 centromeres (Melters et al. 2013; Hartley and O'Neill 2019; Talbert and Henikoff 2020) and thus
101 are considered to be involved in segregation of chromosomes during cell divisions (Henikoff et
102 al. 2001; McKinley and Cheesman 2016). Yet despite their rather conservative function,
103 centromeric satDNAs turn over very fast (Henikoff et al. 2001; Bracewell et al. 2019; Ávila
104 Robledillo et al. 2020; Nishihara et al. 2021). It has been hypothesized that rapid co-evolution of
105 both centromeric DNA and associated proteins is mainly driven by centromere drive (Henikoff
106 et al. 2001). The hypothesis postulates that homologous chromosomes differ in their capability
107 to bind spindle microtubules and thus can segregate non-randomly exploiting the asymmetric
108 female meiosis, which produces three polar bodies (i.e. the evolutionary dead-ends) and only
109 one egg (Henikoff et al. 2001; Kursel and Malik 2018; Kumon and Lampson 2022). Deleterious
110 segregation errors induce selective pressure, which fuels the evolution of involved proteins and
111 DNA repeats, thus suppressing the drive (Henikoff et al. 2001; Kumon and Lampson 2022).

112 Hence, it was hypothesized that the reduction in centromeric clusters of the Nfu-SatA
113 and Nfu-SatB repeats on Y chromosomes observed in *N. furzeri* reflects relaxed selection
114 imposed by centromere drive (Štundlová et al. 2022), as the Y chromosome never passes
115 through female meiosis (cf. Yoshida and Kitano 2012; Pokorná et al. 2014). Unfortunately,
116 nothing is known about killifish centromeric organization outside *N. furzeri* and *N. kadleci*
117 (Reichwald et al. 2009, 2015; Štundlová et al. 2022) and little is known about the centromere
118 organization in teleost fishes in general. Rather than identifying sequences which bind
119 centromeric proteins (Cech and Peichel 2016; Ichikawa et al. 2017), the available studies have
120 focused mainly on sequences associated with centromeres, detected either by molecular or
121 bioinformatic methods and physically mapped by means of *in situ* hybridization (Ferreira et al.
122 2010; Suntronpong et al. 2020; Stornioli et al. 2021; Goes et al. 2022, 2023; Kretschmer et al.
123 2022). More recently, these sequences have been inferred directly from long read sequencing
124 data (Ichikawa et al. 2017; Conte et al. 2019; Varadharajan et al 2019; Tao et al. 2021). These
125 are typically satellite sequences presumably containing conserved motifs such as the CENP-B
126 box needed for chromosome stability and cell division (Suntronpong et al. 2016; Gamba and
127 Fachinetti 2020). Centromeric tandem repeats seem to be homogenized at higher rates in
128 teleost fishes compared to other vertebrates (Suntronpong et al. 2020) and their evolutionary

dynamics seems to reflect centromeric position with those of acrocentrics being more conserved (Ichikawa et al. 2017).

In the present study, we analyzed repetitive sequences across the representatives of *Nothobrachnius* genus by means of RepeatExplorer2 bioinformatic pipeline (Novák et al. 2020) to identify repeats associated with centromeric regions and to look for evidence of centromere drive. Our results suggest that Nfu-SatA and Nfu-SatB are associated with centromeres only in one lineage of the Southern clade, although Nfu-SatB can be detected also in representatives of the Coastal clade, in agreement with the "library" hypothesis (i.e. the existence of shared collection of satDNA repeats among related species, with varied degree of their amplification and contraction; Fry and Salser 1977; Ruiz-Ruano et al. 2016). We also identified novel repeat associated with centromeres in the Coastal-clade species. Based on the presence of larger (peri)centromeric heterochromatin blocks observed in the Southern-clade species but not in other studied representatives, we discuss a possible reversal of spindle orientation in the common ancestor of this clade.

2. Materials and Methods

2.1 Fish sampling

We analyzed individuals of 14 species representing the Southern and Coastal clade (seven and five species, respectively) of the genus *Nothobranchius*, with *N. ocellatus* and *Fundulosoma thierryi* as their outgroups. The studied individuals from *N. orthonotus*, *N. kuhntae*, *N. pienaari*, *N. rachovii*, *N. eggersi* and *N. rubripinnis* were sampled from laboratory populations recently derived from wild-caught individuals and were previously identified based on morphology and the phylogenetic analysis of mitochondrial and nuclear DNA markers (for details, see Bartáková et al. 2015; Blažek et al. 2017; Reichard et al. 2022). The remaining species were obtained from specialists and experienced hobby breeders who keep strictly population-specific lineages derived from original imports. In this case, the species identity was confirmed on the basis of key morphological characters (Wildekamp 1996, 2004; Watters et al. 2008, 2020; Nagy 2018). The detailed information is provided in Table 1.

163

164 **Table 1** List of *Nothobranchius* killifish species used in this study along with their sample sizes
165 (N) and origin

Clade	Species	Code	N*	Source / locality
outgroup	*Fundulosoma thierryi* Ahl, 1924	FTH	1♂, 3♀	aquarium strain
Southern clade	*Nothobranchius furzeri* Jubb, 1971	NFU	1♂, 1♀	Chefu, MZ
	N. kadleci Reichard, 2010	NKA	1♂, 1♀	Gorongosa, MZ
	N. orthonotus (Peters, 1844)	NOR	3♂, 3♀	Limpopo, MZ
	N. kuhntae (Ahl, 1926)	NKU	4♂, 3♀	Pungwe, MZ
	N. pienaari Shidlovskyi, Watters & Wildekamp, 2010	NPI	2♂, 3♀	Limpopo, MZ
	N. krysanovi Shidlovskyi, Watters & Wildekamp, 2010	NKR	2♂, 2♀	Quelimane, MZ
	N. rachovii Ahl, 1926	NRA	2♂, 2♀	Beira Airport, MZ
Ocellatus clade	*N. ocellatus* (Seegers, 1985)	NOC	1♂, 1♀	Nyamwage, TZ
Coastal clade	*N. eggersi* Seegers, 1982	NEG	2♂, 1♀	Bagamoyo, TZ
	N. foerschi Wildekamp & Berkenkamp, 1979	NFO	2♂	Soga, TZ
	N. guentheri (Pfeffer, 1983)	NGU	4♂, 3♀	Zanzibar, TZ
	N. cardinalis Watters, Cooper & Wildekamp, 2008	NCA	1♂	Matandu, TZ
	N. rubripinnis Seegers, 1986	NRU	2♂, 2♀	Kitonga, TZ

166 * number and sex of individuals used for each method is specified in Supplementary Table 1
167

168 **2.2 Chromosomal preparations**

169 Mitotic chromosome spreads were obtained either i) from regenerating caudal fin tissue (Völker
170 and Ráb 2015) with modification described in Sember et al. (2015) and a fin regeneration time
171 ranging from one to two weeks, or ii) by a direct preparation from the cephalic kidney following
172 Ráb and Roth (1988) and Kligerman and Bloom (1977), with in the latter protocol being
173 modified according to Krysanov and Demidova (2018). In the kidney-derived preparations, the
174 chromosomal spreading quality was enhanced using a dropping technique by Bertollo et al.
175 (2015). Preparations were inspected with phase-contrast optics and those of sufficient quality
176 were dehydrated in an ethanol series (70%, 80%, and 96%, 2 min each) and stored at -20 °C
177 until use.
178

179 **2.3 Constitutive heterochromatin staining**

180 Analysis of constitutive heterochromatin distribution was done by C-banding (Haaf and Schmid
181 1984), using 4′,6-diamidino-2-phenolindole (DAPI) (1.5 µg/mL in anti-fade; Cambio, Cambridge,
182 UK) counterstaining. Fluorescent staining with the GC-specific fluorochrome Chromomycin A_3
183 (CMA_3) and the AT-specific fluorochrome DAPI (both Sigma-Aldrich, St. Louis, MO, USA) was
184 performed according to Mayr et al. (1985) and Sola et al. (1992).
185

186 **2.4 Whole-genome sequencing data**

187 Genomic DNA was sequenced *de novo* in *Nothobranchius guentheri*, *N. kadleci*, *N. orthonotus*,
188 *N. rachovii* and *N. rubripinnis*. First, high molecular weight genomic DNA (HMW gDNA) was
189 extracted from three females of each species using a MagAttract HMW DNA Kit (Qiagen,
190 Hilden, Germany), following the provided protocol. Next, Illumina paired-end libraries with 450
191 bp insert size were prepared from the isolated HMW gDNA and sequenced on the NovaSeq
192 6000 platform at Novogene (HK) Co., Ltd. (Hong Kong, China), yielding, at least, 5 Gb (ca 3.3×
193 coverage of *Nothobranchius furzeri* genome; 1C = 1.54 Gb, Reichwald et al. 2009). Resulting
194 data were deposited into the Sequence Read Archive (SRA) under accession numbers XXX –
195 XXX. In *N. furzeri*, sequencing data from three female specimen were obtained from the SRA
196 (accession numbers ERR583470, ERR58471, SRR1261480; Reichwald et al. 2015).
197
198 **2.5 Analysis of repetitive DNA**
199 The satellitome was characterized using RepeatExplorer2 (Novák et al. 2020). Prior to the
200 analysis, the quality of raw Illumina reads was checked using FastQC (version 0.11.5; Andrews
201 2010). Low quality reads and adapter sequences were removed using cutadapt (version 1.15;
202 Martin 2011) with settings for two-color chemistry: '--nextseq-trim=20 -u -50 -U -50 -m 100 -a
203 AATGATACGGCGACCACCGAGATCTACACTCTTTCCCTACACGACGCTCTTCCGATCT -A
204 GATCGGAAGAGCACACGTCTGAACTCCAGTCACNNNNNNATCTCGTATGCCGTCTTCTGC
205 TTG'. For comparative analysis, 1,600,000 reads (ca 0.1× genome coverage of *N. furzeri*) were
206 pseudorandomly subsampled from each biological replica of each species and resulting
207 subsets were concatenated and analyzed together. The RepeatExplorer2 pipeline was run on
208 the Galaxy server (The Galaxy Community 2022) with Metazoa version 3.0 protein domain
209 database and automatic filtering of abundant repeats. In addition, the repeats were studied in
210 each species independently, using a set of 7,125,000 reads (ca 0.5× coverage) and equivalent
211 RepeatExplorer2 parameters. Calculation of G+C content and reciprocal BLAST were
212 performed in GeneiousPrime (version 2020.1.2; https://www.geneious.com). To target potential
213 centromeric repeats, the results of the single-species analysis were confined to high confidence
214 satellites with estimated abundance in the genome at least 0.15% and monomer length <1kb
215 only.
216
217 **2.6 Identification of putative CENP-B box**
218 SatDNA motifs with confirmed centromeric localization (see below) were manually inspected for
219 the presence of 17-bp-long CENP-B box motif (Suntronpong et al. 2016) using Geneious
220 Prime. Alignment of putative CENP-B sequences from human (*Homo sapiens*; Masumoto et al.

221 1989), threespine stickleback (*Gasterosteus aculeatus*; Cech and Peichel 2015), ninespine
222 stickleback (*Pungitius pungitius;* Varadharajan et al. 2019), Asian swamp eel (*Monopterus*
223 *albus;* Suntronpong et al. 2020) and turquoise killifish (*Nothobranchius fuzeri*; this work) were
224 performed with a Geneious native algorithm with default settings for global alignment.
225
226 **2.7 Fluorescence in situ hybridization (FISH)**
227
228 **2.7.1. Preparation of FISH probes**
229 We previously characterized Nfu-SatA and Nfu-SatB as the most abundant satellite DNA motifs
230 in *N. furzeri* and *N. kadleci* (Štundlová et al. 2022). For FISH, the probe covering the whole
231 monomer length 77 bp of Nfu-SatA was generated by 5' labeling with Cy3 during synthesis
232 (Generi Biotech, Hradec Králové, Czech Republic). In the same way, the probes for the Cl-36,
233 Cl-127, Cl-260 and Cl-294, characterized for the first time in the present study (see below),
234 have been prepared. In the case of Nfu-SatB (348-bp-long monomer), the clones with inserts
235 containing three adjacent tandemly arrayed Nfu-SatB monomers which were prepared and
236 verified in the previous study (Štundlová et al. 2022) were used for the FISH probe preparation.
237 The entire plasmids were labeled by nick translation using a Cy3 NT Labeling Kit (Jena
238 Bioscience, Jena, Germany). For the final probe mixture preparation, 250–500 ng of labeled
239 plasmid and 12.5–25 µg of sonicated salmon sperm DNA (Sigma-Aldrich) were applied per
240 slide. The final hybridization mixtures for each slide (15 µL) were prepared according to Sember
241 et al. (2015).
242
243 **2.7.2. Standard FISH analysis**
244 Single-color FISH experiments with Nfu-SatB probe were carried out following Sember et al.
245 (2015) (slide pre-treatment, probe/chromosomes denaturation and hybridization conditions) and
246 Yano et al. (2017) (post-hybridization washing), with modifications described in Štundlová et al.
247 (2022). Briefly, following standard pre-treatment steps, chromosomes were denatured in 75%
248 formamide in 2× SSC (pH 7.0) (Sigma-Aldrich) at 72 °C for 3 min. The hybridization mixture
249 was denatured at 86 °C for 6 min. The hybridization took place overnight (17–24h) at 37 °C in a
250 moist chamber. Subsequently, non-specific hybridization was removed twice in 1× SSC (pH
251 7.0) (65 °C, 5 min each) and once in 4× SSC in 0.01% Tween 20 (42 °C, 5 min), followed by
252 washing in 1× PBS (1 min at room temperature; RT). Slides were dehydrated in an ethanol
253 series (70%, 80%, and 96%, 2 min each) and then mounted in anti-fade containing 1.5 µg/mL
254 DAPI (Cambio, Cambridge, UK).

255
256 **2.7.3. Non-denaturing FISH (ND-FISH)**
257 Remaining five satDNA probes (Nfu-SatA, Cl-36, Cl-127, Cl-260 and Cl-294; more details
258 provided in section 3.2) were mapped using ND-FISH according to Cuadrado and Jouve (2010)
259 with some modifications. Briefly, a total of 30 µL of hybridization mixture containing 2 pmol/µL
260 of oligonucleotides (labeled at 5' end with Cy3) in 2× SSC were used per slide. Then the
261 mixture was denatured at 80 ºC for 5 min and immediately placed on ice. After that, the
262 denatured hybridization mixture was transferred into the slides with neither pre-treatment steps
263 nor chromosome denaturation. After two hours of hybridization at RT, the slides were washed
264 with 4× SSC 0.2% Tween-20 at RT and shaking for 10 min, followed by 5 min washing in 4×
265 SSC 0.1% Tween-20 also at RT and shaking. Chromosome preparations were then passed
266 through ethanol series (70%, 80% and 96%, 3 min each) and then air dried. Chromosomes
267 were counterstained with 20 µL of DABCO anti-fade (1,4-diazabicyclo(2.2.2)-octane containing
268 0.2 µg/mL DAPI (both Sigma-Aldrich) or in anti-fade containing 1.5 µg/mL DAPI Cambio,
269 Cambridge, UK).
270
271 **2.8. Microscopic analyses and image processing**
272 Images from all cytogenetic methods were captured using a BX53 Olympus microscope
273 equipped with an appropriate fluorescence filter set and coupled with a black and white CCD
274 camera (DP30W Olympus). Images were acquired for each fluorescent dye separately using
275 DP Manager imaging software (Olympus), which was further used also to superimpose the
276 digital images with the pseudocolors (red for CMA_3 and green for DAPI in case of fluorescence
277 staining; blue for DAPI and red for Cy3 in case of FISH). Composite images were then
278 optimized and arranged using Adobe Photoshop, version CS6.
279 At least 20 chromosome spreads per individual and method were analyzed.
280 Chromosomes were classified according to Levan et al. (1964), but modified as m –
281 metacentric, sm – submetacentric, st – subtelocentric, and a – acrocentric, where st and a
282 chromosomes were scored together into st-a category.
283
284 **3. Results**
285
286 **3.1 Cytogenetics**
287 **Basic karyotype characteristics**

288 Individuals from all studied species displayed mostly the same 2n and highly similar proportion
289 of chromosome categories as previously reported (Reichwald et al. 2009, 2015; Krysanov and
290 Demidova 2018). The only exception was *N. ocellatus*, where we recorded 2n = 32 with the
291 karyotype being composed exclusively of monoarmed (st-a) chromosomes, in contrast to
292 previously reported 2n = 30 with one chromosome pair being large metacentric (Krysanov and
293 Demidova 2018). The individuals studied by Krysanov and Demidova (2018) were later found to
294 be members of a newly described closely related species *N. matanduensis* (Watters et al.
295 2020) (S. Simanovsky, pers. commun.). Finally, in line with the previous reports (Ewulonu et al.
296 1985; Krysanov and Demidova 2018), *Fundulosoma thierryi* and *N. guentheri* possessed male
297 heterogametic $X_1X_1X_2X_2/X_1X_2Y$ multiple sex chromosome system manifested by different
298 chromosome counts between males and females (males had one chromosome less) and
299 particularly in *N. guentheri* the male-limited neo-Y chromosome was discernible as the only
300 large sm/st element in the complement.
301
302 **Distribution and composition of constitutive heterochromatin**
303 Amount of constitutive heterochromatin varied among the studied *Nothobranchius* spp.
304 (Supplementary Fig. 1). The outgroup taxon *F. thierryi* together with *Nothobranchius* species
305 from the Southern clade possessed generally more heterochromatin segments than *N.*
306 *ocellatus* and species from the Coastal clade where the narrow C-bands were confined mostly
307 to the (peri)centromeric regions of overwhelming majority (*N. cardinalis, N. ocellatus*), two-
308 thirds (*N. rubripinnis*), about half (*N. eggersi*, *N. guentheri*) or several chromosomes (*N.*
309 *foerschi*) of the complement. Within the chromosome complements of *N. cardinalis*, *N.*
310 *guentheri* and *N. rubripinnis*, the largest metacentric chromosome pair either lacked or had
311 unremarkable/ notably smaller C-bands compared to the remainder of the chromosome set
312 (Supplementary Fig. 1J–M). In *N. foerschi*, the largest metacentric chromosome pair possessed
313 a distinct (peri)centromeric C-band, while the second largest metacentric pair displayed only
314 tiny heterochromatin block (Supplementary Fig. 1I). By contrast, majority of large biarmed
315 chromosomes in species of the Southern clade possessed large heterochromatin segments
316 (see below). In addition to (peri)centromeric bands, heterochromatin accumulations were
317 present on the short arms of several chromosomes in *N. eggersi*. In males of *N. guentheri*, neo-
318 Y sex chromosome bore an apparent C-banded region on its long arms Supplementary Fig. 1J,
319 arrowhead). The other species with known X_1X_2Y multiple sex chromosome system (*F. thierryi*)
320 did not show any exceptional C-banding pattern on these sex chromosomes. Four st-a
321 chromosomes in *F. thierryi* displayed remarkable heterochromatin blocks covering their short

322 arms. In the Southern clade, *N. orthonotus* and *N. kuhntae* featured the highest amount and
323 diversity of heterochromatin blocks which were distributed on multiple regions across the
324 chromosome complement. This observation is consistent with large (peri)centromeric regions
325 found previously in closely related *N. furzeri* and *N. kadleci* (Štundlová et al. 2022; see
326 Supplementary Fig. 2A, B for comparison). On the other hand, chromosomes of *N. pienaari*, *N.*
327 *krysanovi* and *N. rachovii* bore almost exclusively (peri)centromeric bands of variable lengths,
328 some of them being remarkably large (Supplementary Fig. 1D–F). In the species with almost
329 exclusively biarmed (metacentric or submetacentric) chromosomes and low 2n, namely *N.*
330 *krysanovi* and *N. rachovii*, some (peri)centromeres were arranged as two large adjacent blocks.
331 *N. krysanovi* also displayed additional interstitial heterochromatin blocks on several
332 chromosomes. In *N. rachovii* only two large submetacentric chromosomes possessed very tiny
333 interstitial bands in addition to (peri)centromeric ones.
334 Fluorescent staining revealed, besides few predominantly $DAPI^+$ (AT-rich) bands (e.g.,
335 in *F. thierryi*, *N. orthonotus*), variable amount and distribution of CMA_3^+ (GC-rich) regions. Five
336 species (*F. thierryi*, *N. pienaari*, *N. krysanovi* and *N. foerschi*) displayed just one pair of clear
337 terminal or interstitial signals, highly likely overlapping with major ribosomal DNA (rDNA) cluster
338 (cf. Sember et al. 2015 and references therein). Similar signals were revealed also on the neo-
339 Y and at least one X chromosome of *N. guentheri* (Supplementary Fig. 3J). Several *N.*
340 *guentheri* chromosomes also featured additional tiny centromeric signals on at least four
341 chromosomes (Supplementary Fig. 3J, K). In *N. rachovii*, terminal CMA_3^+ signals were
342 observed on the short arms of the smallest acrocentric chromosome pair, and at least four large
343 metacentrics/submetacentrics had a tiny centromeric signal (Supplementary Fig. 3F). *N.*
344 *ocellatus* and *N. eggersi* bore up to seven and up to four signals, respectively. *N. cardinalis* and
345 *N. rubripinnis* shared the CMA_3 pattern in the way that (peri)centromeres of all chromosomes
346 were GC-rich except for the one pair of large metacentric chromosomes. Finally, almost all
347 chromosome pairs in *N. orthonotus* and *N. kuhntae* had GC-rich (peri)centromeres, similarly to
348 patterns found in *N. furzeri* and *N. kadleci* (Štundlová et al. 2022; Supplementary Fig. 2C, D).
349
350 **3.2 Identification of candidate repeats**
351 The comparative analysis of tandem repeats in representatives of the Southern (*N. furzeri*, *N.*
352 *kadleci*, *N. orthonotus*, *N. rachovii*) and Coastal (*N. guentheri*, *N. rubripinnis*) clades revealed in
353 total 21 high confidence satellites with various abundances (Table 2). The two most abundant
354 tandem repeats, namely Cl-11 and Cl-26, were the previously studied putative centromeric
355 repeats Nfu-SatB and Nfu-SatA, respectively. Besides *N. furzeri* and *N. kadleci*, these clusters

356 were also enriched in *N. orthonotus*, however, limited or completely missing in *N. rachovii*, *N.*
357 *guentherii* and *N. rubripinnis*, suggesting existence of different motifs in centromeres of these
358 species. Interestingly, satellites Cl-36 and Cl-294 showed the opposite pattern, as they were
359 present in *N. rubripinnis* and *N. guentherii* but missing in the rest of the surveyed taxa. Single-
360 species analysis with more stringent criteria (estimated abundance in the genome at least
361 0.15%, monomer length <1kb) confirmed these results. Besides already identified markers, one
362 more abundant satDNA (Cl-127) was identified to be shared by multiple species and was
363 therefore included in further analysis, as well as Cl-260, which showed a high number of
364 similarity hits with the above mentioned Nfu-SatA (Cl-26) (Table 3).
365 Intriguingly, we found a putative CENP-B box sequence in Nfu-SatB repeat. Alignment
366 to human CENP-B box sequence showed 0.47 identity, which is similar to other fish species
367 (Supplementary Fig. 4). This finding along with the length of Nfu-SatB motif (348 bp; i.e.
368 approx. twice the length of the nucleosome unit) may imply a possible role of Nfu-SatB in
369 centromere function (Talbert and Henikoff 2020). However, no CENP-B box motif was
370 recovered in other inspected repeats and particularly Cl-36 centromeric satellite of *N. rubripinis*
371 is also too short (48 bp monomer) compared to other repeats with putative centromeric
372 function.
373
374 **Table 2** High confidence satellites identified by comparative analysis with RepeatExplorer2

Satellite	Monomer (bp)	GC (%)	Avg reads per replica						Notes
			NFU	NKA	NOR	NRA	NGU	NRU	
Cl-11	**348**	**41.1**	**2,933**	**1,508**	**643**	**50**	**23**	**9**	**Previously identified Nfu-SatB***
Cl-26	**77**	**63.6**	**560**	**2,533**	**369**	**0**	**2**	**0**	**Previously identified Nfu-SatA***
Cl-28	169	36.1	466	164	4,700	34	18	50	
Cl-36	**48**	**45.8**	**0**	**0**	**0**	**0**	**195**	**2,107**	**Specific for Coastal clade**
Cl-97	93	60.2	398	1,240	262	42	521	233	
Cl-127	**39**	**20.5**	**1,160**	**836**	**19**	**21**	**14**	**28**	**High abundance in multiple species**
Cl-147	349	60.2	62	313	119	108	33	996	
Cl-156	49	65.3	1,261	217	30	0	0	0	
Cl-187	84	31	763	214	86	207	178	68	
Cl-238	24	58.3	556	27	3	2	13	7	
Cl-260	**76**	**57.9**	**0**	**512**	**2**	**0**	**0**	**0**	**Similarity hits with Nfu-SatA (Cl-26)**
Cl-274	662	46.8	1	0	10	163	266	2	
Cl-278	21	19	304	20	56	14	17	18	
Cl-286	20	45	0	0	356	0	1	4	

Cl-294	**63**	**31.7**	**0**	**0**	**0**	**0**	**193**	**137**	**Specific for Coastal clade**
Cl-297	691	42.1	87	46	67	45	35	37	
Cl-310	976	40.1	47	31	40	48	41	61	
Cl-327	980	37.3	49	42	29	37	29	41	
Cl-335	625	43.3	0	0	208	0	0	0	
Cl-342	580	36.9	39	27	29	20	39	39	
Cl-367	490	44.3	27	15	16	29	33	44	

Markers selected for physical mapping are indicated in bold

*Reichwald et al. 2009; Štundlová et al. 2022

Table 3 Species-specific analysis of the most abundant satellites (abundance >0.15% of the genome, monomer length < 1kb)

Species	Cluster	Satellite ID (from comparative analysis)	Estimated genome proportion (%)	Notes
N. furzeri	**NFU-1**	**Cl-11**	**16**	**Previously identified Nfu-SatB***
	NFU-12	**Cl-26**	**3.5**	**Previously identified Nfu-SatA***
	NFU-7	**Cl-127**	**0.48**	
	NFU-8	Cl-156	0.47	
	NFU-29	Cl-238	0.27	
N. kadleci	**NKA-1**	**Cl-26**	**9.6**	**Previously identified Nfu-SatA***
	NKA-2	**Cl-11**	**7.5**	**Previously identified Nfu-SatB***
	NKA-15	Cl-97	0.48	
	NKA-34	**Cl-127**	**0.34**	
N. orthonotus	**NKA-59**	**Cl-11**	**2.3**	**Previously identified Nfu-SatB***
	NKA-1	Cl-28	2.2	
	NKA-24	**Cl-26**	**0.41**	**Previously identified Nfu-SatA***
N. rachovii	No satellites fitting the criteria were identified			
N. guentheri	**NGU-94**	**Cl-36**	**0.18**	
N. rubripinnis	**NRU-1**	**Cl-36**	**2**	
	NRU-23	Cl-147	0.37	

Markers selected for physical mapping are indicated in bold

*Reichwald et al. 2009; Štundlová et al. 2022

3.3 Physical mapping of satDNA

FISH with Nfu-SatA (Cl-26) probe revealed detectable clusters only in *N. orthonotus* and *N. kuhntae* (Supplementary Fig. 5B–D). All signals were restricted to (peri)centromeric regions of almost all chromosomes, corroborating patterns found in *N. furzeri* and *N. kadleci* (Štundlová et al. 2022; Supplementary Fig. 2E, F). Whilst all *N. kuhntae* individuals shared the same pattern

388 (i.e., all but one chromosome pair carrying the signal; Supplementary Fig. 5D), individuals of *N.*
389 *orthonotus* displayed site-number variability, with the number of chromosomes lacking the
390 signal being either four (1 male), five (1 male, 1 female), or six (two males, one female)
391 chromosomes (Supplementary Fig. 5B–C).

392 Detectable clusters of Nfu-SatB (Cl-11) were found in (peri)centromeric regions of all
393 chromosomes in *N. orthonotus*, *N. kuhntae* (i.e. the same pattern as in *N. furzeri* and *N.*
394 *kadleci*; Štundlová et al. 2022 and Supplementary Fig. 2G, H), and in (peri)centromeric or
395 terminal regions of about one-third of the chromosome complement in *N. pienaari*
396 (Supplementary Fig. 6B–D). Besides these species of Southern clade, we also found clear
397 hybridization patterns in three species of Coastal clade. Individuals of *N. eggersi* showed four
398 signals placed terminally on short arms of st-a chromosomes. *N. foerschi* and *N. cardinalis*
399 each carried one pair of st-a chromosomes with (peri)centromeric signals. The pair was small-
400 sized in *N. cardinalis* and among the largest in *N. foerschi*. The Nfu-SatB loci in *N. foerschi*
401 coincided with CMA_3^+ sites (compare Supplementary Figs 3I and 6I).

402 Satellite repeat Cl-36 was detected only in three species of Coastal clade: *N. rubripinnis*
403 (from which it was isolated), *N. foerschi* and *N. guentheri* (Supplementary Fig. 7K, L, N). The
404 repeat clusters were located exclusively in the (peri)centromeric regions but none of the
405 mentioned species possessed them in all chromosomes. Studied *N. foerschi* and *N. guentheri*
406 males displayed 12 and 16 signals, respectively (Supplementary Fig. 7K, L). In *N. rubripinnis*,
407 22 out of 36 chromosomes bore the signal (Supplementary Fig. 7N).

408 The second satellite limited to *N. rubripinnis* and *N. guentheri* (Cl-294) was hybridized in
409 both these species, however, signals were detected only on the long arms of four
410 chromosomes in *N. rubripinnis* (Supplementary Fig. 8A, B). The lack of signal in *N. guentheri*
411 could be explained either by its abundance being below the FISH detection threshold, or by
412 different organization of this repeat in the genome.

413 Cl-127, shared by *N. furzeri* and *N. kadleci,* was present in both sexes of these species,
414 but no positive FISH signals were observed in *N. orthonotus* (Supplementary Fig. 8C–E). In
415 both species, signals were localized in the long arm of two pairs of chromosomes in both males
416 and females.

417 The last hybridized marker was Cl-260, bearing similarity hits with Nfu-SatA (Cl-26).
418 Positive signals from this satDNA were observed in all centromeres in both sexes of *N. furzeri*
419 and *N. kadleci*. The only difference in the signal pattern between these two species was related
420 to additional prominent signals located terminally on the short arms of two (*N. furzeri*) and four
421 (*N. kadleci*) chromosomes, respectively (Supplementary Fig. 8F, G).

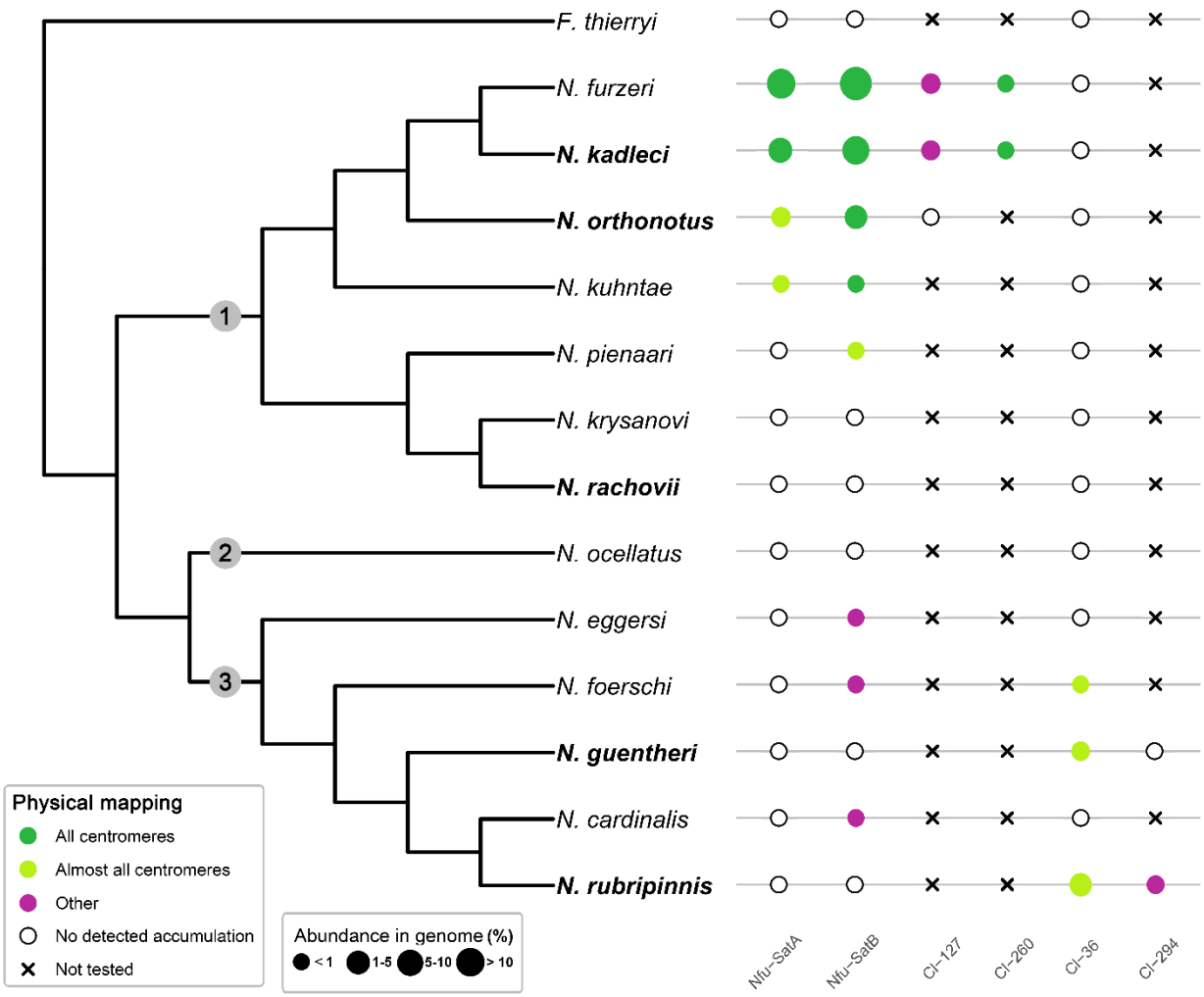

Fig. 1 Phylogenetic relationships and patterns of selected repetitive DNA in inspected *Nothobranchius* species. Simplified phylogenetic tree is based on van der Merwe et al. (2021). Colored circles represent positive FISH signals in different chromosomal locations. The size of the circles reflects the abundance in the genome for respective satDNA. Abundance in the genome (%) is set as ranges. Lack of positive signals after FISH is demarcated by empty circles. Black crosses indicate that a given satDNA was not physically mapped in the particular species. Note that abundance in the genome might not perfectly correlate with chromosomal distribution revealed by physical mapping, because some portion of respective tandem repeats may be present in low-copy clusters undetectable by FISH. Species which were subject to RepeatExplorer2 analysis are shown in bold. Numbers in grey circles in the phylogenetic tree denote distinct *Nothobranchius* clades: 1) Southern Clade; 2) Ocellatus Clade; 3) Coastal Clade

438 **4. Discussion**

439 In the present study, we performed comparative cytogenetic and bioinformatic analyses of
440 satellite DNA across the species of Southern and Coastal clade of the killifish genus
441 *Nothobranchius* to reveal dynamics of repeats associated with centromeres and possible role of
442 meiotic drive in their turnover.

443 Our results showed that the outgroup *F. thierryi* as well as *Nothobranchius* spp. of the
444 Southern clade, namely *N. orthonotus*, *N. kuhntae*, *N. pienaari*, and *N. rachovii*, have in general
445 more C-banded heterochromatin than representatives of the Coastal clade and their outgroup
446 *N. ocellatus.* The presence of extended C-banded (peri)centromeric heterochromatin regions in
447 large metacentric chromosomes of *N. pienaari*, *N. krysanovi* and *N. rachovii* (Supplementary
448 Fig. 1D–F) is consistent with our previous findings in the remaining Southern-clade species, *N.*
449 furzeri and *N. kadleci* (Štundlová et al. 2022 and Supplementary Fig. 2A, B) where we reported
450 large amounts of (peri)centromeric heterochromatin in almost all chromosomes of the
451 complement. By contrast, our present study shows only narrow C-bands in (peri)centromeric
452 regions of majority of chromosomes in *N. cardinalis*, *N. ocellatus,* and *N. rubripinnis*
453 (Supplementary Fig. 1G, L, M), and in about half-to-several chromosomes in *N. eggersi*, *N.*
454 *foerschi* and *N. guentheri* (Supplementary Fig. 1H–J). Interestingly, with the sole exception of
455 one chromosome pair in *N. foerschi*, large metacentric chromosomes originating from fusions
456 either lacked or had unremarkable or notably smaller C-bands than other chromosomes in
457 Coastal-clade species (*N. cardinalis*, *N. foerschi*, *N. guentheri* and *N. rubripinnis*). These
458 findings indicate differences in mechanisms underpinning direction of karyotype change
459 between Southern-clade and Coastal-clade killifishes.

460 To characterize the satDNA evolution, we sequenced and analyzed short reads of *N.*
461 *guentheri*, *N. kadleci*, *N. orthonotus*, *N. rachovii* and *N. rubripinnis* together with data available
462 for the model species *N. furzeri*. In total, the RepeatExplorer2 comparative analysis revealed 21
463 satellite sequences. We have analyzed the distribution of the most abundant satellites in all
464 species (Nfu-SatA, Nfu-SatB, Cl-36 and Cl-127) and two additional markers (Cl-260 sharing
465 similary with Nfu-SatA and Cl-294 specific for the Coastal clade) across both clades and the
466 outgroups by FISH.

467 Štundlová et al. (2022) reported two satDNA motifs, Nfu-SatA and Nfu-SatB,
468 previously identified in the *N. furzeri* strains (Reichwald et al. 2009, 2015) to be the most
469 abundant repeat types in both the *N. furzeri* and *N. kadleci* genomes. Both Nfu-SatA and Nfu-
470 SatB were mapped to (peri)centromeric constitutive heterochromatin blocks of varying sizes in

471 these two sister species (see also Supplementary Fig. 2 C–F). Our results suggest that Nfu-
472 SatA is restricted only to the *N. furzeri* lineage as it is present, although in lower abundance,
473 also in (peri)centromeric regions of almost all chromosomes in *N. orthonotus* and *N. kuhntae*
474 (Supplementary Fig. 5B–D). Lastly, the satellite Cl-260, was detected in the (peri)centromeric
475 regions of all chromosomes in *N. furzeri* and *N. kadleci* only (Supplementary Fig. 8F, G). While
476 Cl-260 is highly likely a new sequence variant of Nfu-SatA, specific for *N. kadleci* genome only
477 (Table 2), its high sequence similarity with Nfu-SatA was apparently responsible for observing a
478 positive hybridization also in (peri)centromeres of *N. furzeri*.

479 Nfu-SatB was also detected in (peri)centromeric regions of all chromosomes in *N.*
480 *orthonotus* and *N. kuhntae* (Supplementary Fig. 6B, C). However, it was further present in
481 detectable amounts also in *N. pienaari* as well as *N. eggersi*, *N. foerschi*, and *N. cardinalis* of
482 the Coastal clade (Supplementary Fig. 6D, H, I, K). The Nfu-SatB signals were located
483 terminally on the short arms of two chromosome pairs in *N. eggersi*, while they resided in
484 (peri)centromeric regions of about one-third of the complement in *N. pienaari* and one
485 chromosome pair of each *N. foerschi* and *N. cardinalis*. Observed pattern is consistent with the
486 "library" hypothesis (Fry and Salser 1977; Ruiz-Ruano et al. 2016) as Nfu-SatB seems to be
487 shared across *Nothobranchius* spp. but it got amplified and associated with centromeres in the
488 *N. furzeri* lineage of the Southern clade.

489 While Nfu-SatA and Nfu-SatB were found restricted to Southern clade species,
490 satellites Cl-36 and Cl-294 mirrored this pattern as they were detected in the Coastal clade
491 only. The Cl-294 was localized on the long arms of only four chromosomes in *N. rubripinnis* and
492 could not have been detected by FISH on chromosomes of *N. guentheri* (Supplementary Fig.
493 8A, B). However, Cl-36 was successfully mapped in three representatives of the Coastal clade
494 (Supplementary Fig. 7K, L, N). The hybridization signals were detected exclusively in the
495 (peri)centromeric regions of majority but not all chromosomes in *N. rubripinnis, N. foerschi*, and
496 *N. guentheri.* Corroborating the C- and fluorescent-banding patterns, Cl-36 clusters were
497 absent in (peri)centromeres of some large metacentric chromosomes (Supplementary Fig. 7K,
498 N). This observation is analogous to previously reported satellite-free centromeres, which
499 emerged upon Robertsonian fusions in zebras (Cappelletti et al. 2022).

500 Interestingly, none of the above tested markers was detected in centromeres of *N.*
501 *rachovii* (Supplementary Figs. 3F, 5F, 6F, 7H) and the RepeatExplorer2 analysis failed to
502 identify any potentially centromeric satellites in this species (Tab. 2, Tab. 3). Since blocks of
503 (peri)centromeric heterochromatin (Supplementary Fig. 1F), visible on most *N. rachovii*
504 chromosomes, suggest the presence of tandem arrays rather than satellite-free centromeres, a

505 possible explanation might be that microsatellites are the involved sequences in this case.
506 Centromeric localization of short repeat motifs has been described before in various organisms
507 (e.g. Kim et al. 2002; Chang et al. 2008) and their presence could escape RepeatExplorer2
508 analysis as this tool is known to omit low complexity sequences (Novák et al. 2020).

509 Furthermore, a putative CENP-B box motif was identified in Nfu-SatB centromeric
510 satellite. As in other fish species, its sequence showed overall 0.47 identity to the human
511 CENP-B box (Supplementary Fig. 4). However, different nucleotide positions are conserved in
512 various fishes (Cech and Peichel 2015; Varadharajan et al. 2019; Suntronpong et al. 2020). In
513 addition, the CENP-B motif was not recovered in any other killifish (peri)centromeric satellites,
514 including Cl-36. Thus, further research is needed to assess the contribution of Nfu-SatB-linked
515 CENP-B box-like motif to centromere function. Differences between X- and Y-linked
516 (peri)centromeric heterochromatin comprising Nfu-SatA and Nfu-SatB were reported in *N.*
517 *furzeri* and *N. kadleci*, with the Y-linked heterochromatin being considerably reduced
518 (Štundlová et al. 2022). It was hypothesized that this is due to absence of centromere drive on
519 the Y chromosome as it is never transmitted via female meiosis (cf. Yoshida and Kitano 2012;
520 Pokorná et al. 2014). Identification of putative centromeric repeat in the Coastal clade
521 potentially presents an opportunity to test this hypothesis as *N. guentheri* has a multiple sex
522 chromosome system of the X_1X_2Y type, in which neo-Y and one of the X chromosomes can be
523 identified by CMA_3 staining (Supplementary Fig. 3J). However, FISH with Cl-36 failed to detect
524 any satDNA clusters on both the neo-Y and the CMA_3-positive X chromosome.

525 It was hypothesized that karyotype evolution is driven by meiotic drive in many animal
526 lineages (Pardo-Manuel de Villena and Sapienza 2001; Blackmon et al. 2019), including fishes
527 (Yoshida and Kitano 2012; Molina et al. 2014), particularly by a nonrandom segregation of
528 rearranged chromosome in female meiosis of heterokaryotypes, due to inherent asymmetry of
529 female meiosis and polarity of a meiotic spindle. Stronger spindles should bind bigger
530 centromeres (Chmátal et al. 2014; Akera et al. 2019; Kursel and Malik 2018; Kumon and
531 Lampson 2022). Yet the direction of the nonrandom segregation is not set in stone. Reversals
532 of spindle polarity supposedly occurred in many phylogenetic groups, which could explain
533 differences in trends in karyotype evolution between related taxa (Pardo-Manuel de Villena and
534 Sapienza 2001; Yoshida and Kitano 2012; Blackmon et al. 2019). It is tempting to speculate
535 that in *N. furzeri* and *N. kadleci*, the egg has a stronger spindle pole than in the other species
536 under study, as they have considerably larger (peri)centromeric heterochromatin blocks
537 comprising Nfu-SatA and Nfu-SatB in all chromosomes but the Y chromosome. Interestingly, in
538 both *N. furzeri* and *N. kadleci* the large blocks of (peri)centric heterochromatin coincide with

539 higher numbers of chromosome arms, but not with different number of chromosomes than
540 expected when compared to karyotypes of other *Nothobranchius* spp. (Krysanov and Demidova
541 2018). It suggests that evolution of satellite DNA in *Nothobranchius* species is associated either
542 with intrachromosomal rearrangements or centromere repositioning, i.e. inactivation of an
543 existing centromere and de novo formation of a new one elsewhere on the chromosome (cf.
544 Amor et al. 2004; Cappelletti et al. 2022).
545 To conclude, our cytogenetic and bioinformatic data suggests that centromere drive
546 operates in *Nothobranchius* killifishes and shape their karyotypes. Reversal of spindle polarity
547 probably occurred in the Southern clade and changed direction of the drive. Further research is
548 needed to parse causes and consequences of karyotype evolution in the killifishes.
549
550 **Acknowledgements:** We would like to thank B. Nagy, A. Nikiforov and H. Hengstler for
551 providing part of the study material and A. Nikiforov for his help in breeding and keeping fishes.
552 We are also grateful to P. Šejnohová for the laboratory assistance.
553
554 **Authors' contributions:** Conceptualization: AS, PN; Data curation: PN, AV, PM, MA; Formal
555 analysis: PN, AV; Funding acquisition: AS; Investigation: AV, KL, PM, TP, MA, JŠ, ŠP, SAS,
556 MJ, PN, AS; Methodology: AS, PN, AV, PM; Project administration: AS, PN; Resources: AS,
557 PN, MR; Supervision: AS, PN, MR; Validation: AV, PM, AS, PN, MA; Writing original draft: AV,
558 AS, PN, PM; Writing—review & editing: PN, AS, AV, PM, MA, JŠ, MR, SAS.
559
560 **Funding:** This study was supported by The Czech Science Foundation (grant no. 19-22346Y
561 (JŠ, PN, KL, AV, TP, MA, ŠP, MJ, AS) and further by RVO:67985904 of IAPG CAS, Liběchov
562 (Czech Academy of Sciences) (MA, ŠP, AS), the Charles University Research Centre program
563 No. 204069 (MA) and “Convocatoria de Recualificación del Sistema Universitario Español-
564 Margarita Salas” postdoctoral grant of University of Jaén, under the “Plan de Recuperación
565 Transformación” program funded by the Spanish Ministry of Universities with European Union’s
566 NextGenerationEU funds (grant no. UJAR10MS) (PM). Computational resources were supplied
567 by the project "e-Infrastruktura CZ" (e-INFRA LM2018140) provided within the program Projects
568 of Large Research, Development and Innovations Infrastructures and the ELIXIR-CZ project
569 (LM2018131), part of the international ELIXIR infrastructure. The funders had no role in study
570 design, data collection and analysis, decision to publish, or preparation of the manuscript.
571

572 **Availability of data and material:** The following nucleotide sequences were deposited in
573 Sequence Read Archive (SRA): XXX. All other relevant data are within the paper and its
574 Supporting Information file.
575
576 **Declarations**
577
578 **Conflicts of interest/Competing interests:** The authors declare that they have no conflict of
579 interest.
580
581 **Ethics approval**: To prevent fish suffering, all handling of fish individuals followed European
582 standards in agreement with §17 of the Act No. 246/1992 Coll. The procedures involving fishes
583 were supervised by the Institutional Animal Care and Use Committee of the Institute of Animal
584 Physiology and Genetics CAS, v.v.i., and the supervisor's permit number CZ 02361 was
585 certified and issued by the Ministry of Agriculture of the Czech Republic. The experiments with
586 *N. foerschi* and *N. cardinalis* were approved by the Ethics Committee of Severtsov Institute of
587 Ecology and Evolution (Order No. 27 of November 9, 2018). For direct preparations of
588 chromosomes from the kidney, fishes were euthanized using 2-phenoxyethanol (Sigma-Aldrich)
589 before organ sampling. Fin samples (a narrow strip of the caudal fin) were taken from live
590 individuals after fishes were anesthetized using MS-222 (Merck KGaA, Darmstadt, Germany).
591
592 **Abbreviations**

2n	diploid chromosome number
a	acrocentric chromosome
CMA_3	Chromomycin A_3
DABCO	1,4-diazabicyclo(2.2.2)-octane
DAPI	4',6-diamidino-2-phenylindole
FISH	fluorescence *in situ* hybridization
gDNA	genomic DNA
m	metacentric chromosome
ND-FISH	non-denaturing FISH
p-arm	short chromosome arm
PBS	phosphate-buffered saline
q-arm	long chromosome arm
rDNA	ribosomal DNA
RT	room temperature
satDNA	satellite DNA
SRA	Sequence Read Archive
SSC	saline-sodium citrate
st	subtelocentric chromosome

611 **6. References**
612
613 Akera T, Trimm E, Lampson MA (2019) Molecular strategies of meiotic cheating by selfish
614 centromeres. Cell 178:1132–1144. https://doi.org/10.1016/j.cell.2019.07.001
615
616 Amor DJ, Bentley K, Ryan J, Perry J, Wong L, Slater H, Choo KA (2004) Human centromere
617 repositioning "in progress". Proc Natl Acad Sci USA 101:6542–6547.
618 https://doi.org/10.1073/pnas.030863710
619
620 Andrews S (2010) FastQC: a quality control tool for high throughput sequence data [Online].
621 http://www.bioinformatics.babraham.ac.uk/projects/fastqc/

622 Ávila Robledillo L, Neumann P, Koblížková A, Novák P, Vrbová I, Macas J (2020) Extraordinary
623 sequence diversity and promiscuity of centromeric satellites in the legume tribe Fabeae. Mol
624 Biol Evol 37:2341–2356. https://doi.org/10.1093/molbev/msaa090

625 Bartáková V, Reichard M, Blažek R, Polačik M, Bryja J (2015) Terrestrial fishes: rivers are
626 barriers to gene flow in annual fishes from the African savanna. J Biogeogr 42:1832–1844.
627 https://doi.org/10.1111/jbi.12567

628 Berois N, García G, de Sá, RO, editors. Annual fishes: life history strategy, diversity and
629 evolution. Boca Raton, FL: CRC Press; 2016.

630 Blackmon H, Justison J, Mayrose I, Goldberg EE (2019) Meiotic drive shapes rates of
631 karyotype evolution in mammals. Evolution 73:511–523. https://doi.org/10.1111/evo.13682

632 Blažek R, Polačik M, Kačer P, Cellerino A, Řežucha R, Methling C, Tomášek O, Syslová K,
633 Terzibasi Tozzini E, Albrecht T et al (2017) Repeated intraspecific divergence in life span and
634 aging of African annual fishes along an aridity gradient. Evolution 71:386–402.
635 https://doi.org/10.1111/evo.13127

636 Blažek R, Polačik M, Reichard M (2013) Rapid growth, early maturation and short generation
637 time in African annual fishes. Evodevo 4:1–7. https://doi.org/10.1186/2041-9139-4-24

638 Bertollo LAC, Cioffi MB, Moreira-Filho O (2015) Direct chromosome preparation from
639 freshwater teleost fishes. In: Ozouf-Costaz C, Pisano E, Foresti F, and de Almeida-Toledo LF
640 (eds) Fish cytogenetic techniques: ray-fin fishes and chondrichthyans. CRC Press, Inc,
641 Endfield, pp 21–26. https://doi. org/ 10. 1201/ b18534-4

642 Bracewell R, Chatla K, Nalley MJ, Bachtrog D (2019) Dynamic turnover of centromeres drives
643 karyotype evolution in drosophila. Elife 8:1–47. https://doi.org/10.7554/eLife.49002

644 Cappelletti E, Piras FM, Sola L, Santagostino M, Abdelgadir WA, Raimondi E, Lescai F,
645 Nergadze SG, Giulotto E (2022) Robertsonian fusion and centromere repositioning contributed
646 to the formation of satellite-free centromeres during the evolution of zebras. Mol Biol Evol 39:1–
647 21. https://doi.org/10.1093/molbev/msac162

648 Cech JN, Peichel CL (2015) Identification of the centromeric repeat in the threespine
649 stickleback fish (*Gasterosteus aculeatus*). *Chromosome Res* 23:767–779.
650 https://doi.org/10.1007/s10577-015-9495-3

651 Cech JN, Peichel CL (2016) Centromere inactivation on a neo-Y fusion chromosome in
652 threespine stickleback fish. Chromosome Res 24:437–450. https://doi.org/10.1007/s10577-016-
653 9535-7

654 Cellerino A, Valenzano DR, Reichard M (2016) From the bush to the bench: the annual
655 *Nothobranchius* fishes as a new model system in biology. Biol Rev 91:511–533.
656 https://doi.org/10.1111/brv.12183

657 Chang SB, Yang TJ, Datema E, Van Vugt J, Vosman B, Kuipers A, Meznikova M, Szinay D,
658 Klein Lankhorst R, Jacobsen E, de Jong H (2008) FISH mapping and molecular organization of
659 the major repetitive sequences of tomato. Chromosome Res 16:919–933.
660 https://doi.org/10.1007/s10577-008-1249-z

661 Chaves R, Adega F, Heslop-Harrison JS, Guedes-Pinto H, Wienberg J (2003). Complex
662 satellite DNA reshuffling in the polymorphic t (1; 29) Robertsonian translocation and
663 evolutionarily derived chromosomes in cattle. Chromosome Res 11:641–648.
664 https://doi.org/10.1023/A:1025952507959

665 Chmátal L, Gabriel SI, Mitsainas GP, Martínez-Vargas J, Ventura J, Searle JB, Schultz RM,
666 Lampson MA (2014) Centromere strength provides the cell biological basis for meiotic drive
667 and karyotype evolution in mice. Curr Biol 24:2295–2300.
668 https://doi.org/10.1016/j.cub.2014.08.017

669 Conte MA, Joshi R, Moore EC, Nandamuri SP, Gammerdinger WJ, Roberts RB, Carleton KL,
670 Lien S, Kocher T (2019) Chromosome-scale assemblies reveal the structural evolution of
671 African cichlid genomes. Gigascience 8:1–20. https://doi.org/10.1093/gigascience/giz030

672 Cuadrado Á, Jouve N (2010) Chromosomal detection of simple sequence repeats (SSRs) using
673 nondenaturing FISH (ND-FISH). Chromosoma 119, 495–503. https://doi.org/10.1007/s00412-
674 010-0273-x

675 Cui R, Medeiros T, Willemsen D, Iasi LNM, Collier GE, Graef M, Reichard M, Valenzano DR
676 (2019) Relaxed selection limits lifespan by increasing mutation load. Cell 178:385–399.e20.
677 https://doi.org/10.1016/j.cell.2019.06.004

678 Ewulonu UK, Haas R, Turner B (1985) A multiple sex chromosome system in the annual killfish,
679 *Nothobranchius guentheri*. Copeia 2:503–508. https://doi.org/10.2307/1444868

680 Ferreira IA, Poletto AB, Kocher TD, Mota-Velasco JC, Penman DJ, Martins C (2010)
681 Chromosome evolution in african cichlid fish: Contributions from the physical mapping of
682 repeated DNAs. Cytogenet Genome Res 129:314–322. https://doi.org/10.1159/000315895

683 Fricke R, Eschmeyer WN, Van der Laan R (eds) (2023) Eschmeyer's catalog of fishes: genera,
684 species, references. http:// resea rchar chive. calac ademy. org/ resea rch/ ichth yology/ catal
685 og/ fishc atmain. asp. Accessed 3 May 2023

686 Fry K, Salser W (1977) Nucleotide sequences of HS-α satellite DNA from kangaroo rat
687 *Dipodomys ordii* and characterization of similar sequences in other rodents. Cell 12:1069–1084.
688 https://doi.org/10.1016/0092-8674(77)90170-2

689 Furness AI (2016) The evolution of an annual life cycle in killifish: adaptation to ephemeral
690 aquatic environments through embryonic diapause. Biol Rev Camb Philos Soc 91:796–812.
691 https://doi.org/10.1111/brv.12194

692 Gamba R, Fachinetti D (2020) From evolution to function: two sides of the same CENP-B coin?
693 Exp Cell Res 390:111959. https://doi.org/10.1016/j.yexcr.2020.111959

694 Garrido-Ramos MA (2017) Satellite DNA: An evolving topic. Genes 8:230.
695 https://doi.org/10.3390/genes8090230

696 Goes CAG, dos Santos RZ, Aguiar WRC, Alves DCV, Silva DMZA. Foresti F, Oliveira C,
697 Utsunomia R, Porto-Foresti F (2022) Revealing the satellite DNA history in *Psalidodon* and
698 *Astyanax* characid fish by comparative satellitomics. Front Genet 13:884072.
699 https://doi.org/10.3389/fgene.2022.884072

700 Goes CAG, dos Santos N, Rodrigues PHM, Stornioli JHF, da Silva AB, dos Santos RZ, Vidal
701 JAD, Silva DMZA, Artoni RF, Foresti F (2023) The satellite DNA catalogues of two
702 Serrasalmidae (Teleostei, Characiformes): conservation of general satDNA features over 30
703 million years. Genes, 14:91. https://doi.org/10.3390/genes14010091

704 Haaf T, Schmid M (1984) An early stage of ZZ/ZW sex chromosomes differentiation in *Poecilia*
705 *sphenops* var. *melanistica* (Poeciliidae, Cyprinodontiformes). Chromosoma 89:37–41.
706 https://doi.org/10.1007/BF00302348

707 Hartley G, O'Neill RJ (2019) Centromere repeats: hidden gems of the genome. Genes 10:223.
708 https://doi.org/10.3390/genes10030223

709 Henikoff S, Ahmad K, Malik HS (2001) The centromere paradox: stable inheritance with rapidly
710 evolving DNA. Science 293:1098–1102. https://doi.org/10.1126/science.1062939

711 Hu CK, Brunet A (2018) The African turquoise killifish: a research organism to study vertebrate
712 aging and diapause. Aging Cell 17:1–15. https://doi.org/10.1111/acel.12757

713 Ichikawa K, Tomioka S, Suzuki Y, Nakamura R, Doi K, Yoshimura J, Kumagai M, Inoue Y,
714 Uchida Y, Irie N, Takeda H, Morishita S (2017) Centromere evolution and CpG methylation
715 during vertebrate speciation. Nat Commun 8:1833. https://doi.org/10.1038/s41467-017-01982-7

716 Kim NS, Armstrong KC, Fedak G, Ho K, Park NI (2002) A microsatellite sequence from the rice
717 blast fungus (*Magnaporthe grisea*) distinguishes between the centromeres of *Hordeum vulgare*
718 and *H. bulbosum* in hybrid plants. Genome 45:165–174. https://doi.org/10.1139/G01-129

719 Kligerman AD, Bloom SE (1977) Rapid chromosome preparations from solid tissues of fishes. J
720 Fish Res Board Can 34:266–269. https://doi.org/10.1139/f77-039

721 Kretschmer R, Goes CAG, Bertollo LAC, Ezaz T, Porto-Foresti F, Toma GA, Utsunomia R,
722 Cioffi MB (2022) Satellitome analysis illuminates the evolution of ZW sex chromosomes of
723 Triportheidae fishes (Teleostei: Characiformes). Chromosoma. https://doi.org/10.1007/s00412-
724 022-00768-1

725 Krysanov E, Demidova T, Nagy B (2016) Divergent karyotypes of the annual killifish genus
726 *Nothobranchius* (Cyprinodontiformes, Nothobranchiidae). Comp Cytogenet 10:439–445.
727 https://doi.org/10.3897/CompCytogen.v10i3.9863

728 Krysanov E, Demidova T (2018) Extensive karyotype variability of African fish genus
729 *Nothobranchius* (Cyprinodontiformes). Comp Cytogenet 12:387–402.
730 https://doi.org/10.3897/CompCytogen.v12i3.25092

731 Krysanov EY, Nagy B, Watters BR, Sember A, Simanovsky SA (2023) Karyotype differentiation
732 in the *Nothobranchius ugandensis* species group (Teleostei, Cyprinodontiformes), seasonal
733 fishes from the east African inland plateau, in the context of phylogeny and biogeography.
734 Comp Cytogenet 7:13–29. https://doi.org/10.3897/compcytogen.v7.i1.97165

735 Kumon T, Lampson MA (2022) Evolution of eukaryotic centromeres by drive and suppression
736 of selfish genetic elements. Semin Cell Dev Biol. https://doi.org/10.1016/j.semcdb.2022.03.026

737 Kursel LE, Malik HS (2018) The cellular mechanisms and consequences of centromere drive.
738 Curr Opin Cell Biol 52:58–65. https://doi.org/10.1016/j.ceb.2018.01.011

739 Levan AK, Fredga K, Sandberg AA (1964) Nomenclature for centromeric position on
740 chromosomes. Hereditas 52:201– 220. https://doi.org/10.1111/j.1601-5223.1964.tb01953.x

741 Mayr B, Ráb P, Kalat M (1985) Localisation of NORs and counterstain-enhanced fluorescence
742 studies in *Perca fluviatilis* (Pisces, Percidae). Genetica 67:51–56.
743 https://doi.org/10.1007/BF02424460

744 Martin M (2011) Cutadapt removes adapter sequences from high-throughput sequencing reads.
745 EMBnet.journal 17:10–12. https://doi.org/10.14806/ej.17.1.200

746 Masumoto H, et al. (1989) A human centromere antigen (CENP-B) interacts with a short
747 specific sequence in alphoid DNA, a human centromeric satellite. J Cell Biol 109:1963 –1973.
748 https://doi.org/10.1083/jcb.109.5.1963

749 McKinley KL, Cheeseman IM (2016). The molecular basis for centromere identity and
750 function. Nat Rev Mol Cell Biol, 17:16–29. https://doi.org/10.1038/nrm.2015.5

751 Melters DP, Bradnam KR, Young HA, Young HA, Telis N, May MR, Ruby JG, Sebra R, Peluso
752 P, Eid J, Rank D et al (2013) Comparative analysis of tandem repeats from hundreds of
753 species reveals unique insights into centromere evolution. Genome Biol 14:R10.
754 https://doi.org/10.1186/gb-2013-14-1-r10

755 Molina WF, Martinez P a., Bertollo LAC, Bidau CJ (2014) Evidence for meiotic drive as an
756 explanation for karyotype changes in fishes. Mar Genomics 15:29–34.
757 https://doi.org/10.1016/j.margen.2014.05.001

758 Nagy B (2018) *Nothobranchius ditte*, a new species of annual killifish from the Lake Mweru
759 basin in the Democratic Republic of the Congo (Teleostei: Nothobranchiidae). Ichthyol Explor
760 Freshw 28:115–134.

761 Nagy B, Watters BR (2021) A review of the conservation status of seasonal *Nothobranchius*
762 fishes (Teleostei: Cyprinodontiformes), a genus with a high level of threat, inhabiting ephemeral
763 wetland habitats in Africa. Aquat Conserv 32: 199–216. https://doi.org/10.1002/aqc.3741

764 Nishihara H, Stanyon R, Tanabe H, Koga A (2021) Replacement of owl monkey centromere
765 satellite by a newly evolved variant was a recent and rapid process. Genes Cells 26:979–986.
766 https://doi.org/10.1111/gtc.12898

767 Novák P, Neumann P, Macas, J (2020) Global analysis of repetitive DNA from unassembled
768 sequence reads using RepeatExplorer2. Nat Protoc 15, 3745–3776.
769 https://doi.org/10.1038/s41596-020-0400-y

770 Pardo-Manuel De Villena F, Sapienza C (2001) Nonrandom segregation during meiosis: The
771 unfairness of females. Mamm Genome 12:331–339. https://doi.org/10.1007/s003350040003

772 Plohl M, Meštrović N, Mravinac B (2012) Satellite DNA evolution. Genome Dyn 7:126–152.
773 https://doi.org/10.1159/000337122

774 Pokorná M, Altmanová M, Kratochvíl L (2014) Multiple sex chromosomes in the light of female
775 meiotic drive in amniote vertebrates. Chromosome Res 22:35–44.
776 https://doi.org/10.1007/s10577-014-9403-2

777 Ráb P, Roth P (1988) Cold-blooded vertebrates. In: Balicek P, Forejt J, Rubeš J (eds) Methods
778 of chromosome analysis. Cytogenetická Sekce Československé Biologické Společnosti při
779 CSAV, Brno, Czech Republic, pp 115–124

780 Reichard M, Giannetti K, Ferreira T, Maouche A, Vrtílek M, Polačik M, Blažek R, Ferreira MG
781 (2022) Lifespan and telomere length variation across populations of wild-derived African
782 killifish. Mol Ecol 31:5979–5992. https://doi.org/10.1111/mec.16287

783 Reichwald K, Lauber C, Nanda I, Kirschner J, Hartmann N, Schories S, Gausmann U, Taudien
784 S, Schilhabel MB, Szafranski K et al (2009) High tandem repeat content in the genome of the

785 short-lived annual fish *Nothobranchius furzeri*: a new vertebrate model for aging research.
786 Genome Biol 10:R16. https://doi.org/10.1186/gb-2009-10-2-r16

787 Reichwald K, Petzold A, Koch P, Downie BR, Hartmann N, Pietsch S, Baumgart M, Chalopin D,
788 Felder M, Bens M et al (2015) Insights into sex chromosome evolution and aging from the
789 genome of a short-lived fish. Cell 163:1527–1538. https://doi.org/10.1016/j.cell.2015.10.071

790 Ruiz-Ruano FJ, López-León MD, Cabrero J, Camacho JPM (2016) High-throughput analysis of
791 the satellitome illuminates satellite DNA evolution. Sci Rep 6:28333.
792 https://doi.org/10.1038/srep28333

793 Sember A, Bohlen J, Šlechtová V, Altmanová M, Symonová R, Ráb P (2015) Karyotype
794 differentiation in 19 species of river loach fishes (Nemacheilidae, Teleostei): extensive
795 variability associated with rDNA and heterochromatin distribution and its phylogenetic and
796 ecological interpretation. BMC Evol Biol 15:251. https://doi.org/10.1186/s12862-015-0532-9

797 Sola L, Rossi AR, Iaselli V, Rasch EM, Monaco PJ (1992) Cytogenetics of bisexual/unisexual
798 species of *Poecilia*. II. Analysis of heterochromatin and nucleolar organizer regions in *Poecilia*
799 *mexicana mexicana* by C-banding and DAPI, quinacrine, chromomycin A_3, and silver staining.
800 Cytogenet Cell Genet 60:229–235. https://doi. org/10.1159/000133346

801 Stornioli JHF, Goes CAG, Calegari RM, dos Santos RZ, Giglio LM, Foresti F, Oliveira C,
802 Penitente M, Porto-Foresti F, Utsunomia R (2021). The B chromosomes of *Prochilodus lineatus*
803 (Teleostei, Characiformes) are highly enriched in satellite DNAs. Cells 10:1527.
804 https://doi.org/10.3390/cells10061527

805 Štundlová, J, Hospodářská M, Lukšíková K, Voleníková A, Pavlica T, Altmanová M, Richter A,
806 Reichard M, Dalíková M, Pelikánová Š, Marta, A, Simanovsky SA, Hiřman M, Jankásek M,
807 Dvořák T, Bohlen J, Ráb P, Englert C, Nguyen P, Sember A (2022) Sex chromosome
808 differentiation via changes in the Y chromosome repeat landscape in African annual killifishes
809 *Nothobranchius furzeri* and *N. kadleci*. Chromosome Res 30:309–33.
810 https://doi.org/10.1007/s10577-022-09707-3

811 Suntronpong A, Kugou K, Masumoto H, Srikulnath K, Ohshima K, Hirai H, Koga A (2016)
812 CENP-B box, a nucleotide motif involved in centromere formation, occurs in a New World
813 monkey. Biol Lett 12:20150817. https://doi.org/10.1098/rsbl.2015.0817

814 Suntronpong A, Singchat W, Kruasuwana W, Prakhongcheep O, Sillapaprayoon S, Muangmai
815 N, Somyong S, Indananda C, Kraichak E, Peyachoknagul S, Srikulnath K (2020)
816 Characterization of centromeric satellite DNAs (MALREP) in the Asian swamp eel (*Monopterus*
817 *albus*) suggests the possible origin of repeats from transposable elements. Genomics
818 112:3097–3107. https://doi.org/10.1016/j.ygeno.2020.05.024

819 Talbert PB, Henikoff S (2020) What makes a centromere? Exp Cell Res 389:111895.
820 https://doi.org/10.1016/j.yexcr.2020.111895

821 Tao W, Xu L, Zhao L, Zhu Z, Wu X, Min Q, Wang D, Zhou Q (2021) High-quality chromosome-
822 level genomes of two tilapia species reveal their evolution of repeat sequences and sex
823 chromosomes. Mol Ecol Resour 21:543–560. https://doi.org/10.1111/1755-0998.13273

824 Terzibasi Tozzini E, Cellerino A (2020) *Nothobranchius* annual killifishes. Evodevo 11:25.
825 https://doi.org/10.1186/s13227-020-00170-x

826 Thakur J, Packiaraj J, Henikoff S (2021) Sequence, chromatin and evolution of satellite DNA.
827 Int J Mol Sci 22:4309. https://doi.org/10.3390/ijms22094309

828 The Galaxy Community (2022) The Galaxy platform for accessible, reproducible and
829 collaborative biomedical analyses: 2022 update. Nucleic Acids Research 50: W345–W351.
830 https://doi.org/10.1093/nar/gkac247

831 van der Merwe PDW, Cotterill FPD, Kandziora M, Watters BR, Nagy B, Genade T, Flügel TJ,
832 Svendsen DS, Bellstedt DU (2021) Genomic fingerprints of palaeogeographic history: the
833 tempo and mode of rift tectonics across tropical Africa has shaped the diversification of the
834 killifish genus *Nothobranchius* (Teleostei: Cyprinodontiformes). Mol Phylogenet Evol
835 158:106988. https://doi.org/10.1016/j.ympev.2020.106988

836 Varadharajan S, Rastas P, Löytynoja A, Matschiner M, Calboli FCF, Guo B, Nederbragt AJ,
837 Jakobsen KS, Merilä J (2019) A high-quality assembly of the nine-spined stickleback (*Pungitius*
838 *pungitius*) genome. Genome Biol Evol 11:3291–3308. https://doi.org/10.1093/gbe/evz240

839 Völker M, Ráb P (2015) Direct chromosome preparation from regenerating fin tissue. In: Ozouf-
840 Costaz C, Pisano E, Foresti F, and de Almeida-Toledo LF (eds) Fish cytogenetic techniques:
841 ray-fin fishes and chondrichthyans. CRC Press, Inc, Endfield, pp 37–41.
842 https://doi.org/10.1201/b18534-4

843 Watters BR, Cooper BJ, Wildekamp RH (2008) Description of *Nothobranchius cardinalis* spec.
844 nov. (Cyprinodontiformes: Aplocheilidae), an annual fish from the Mbwemkuru River basin,
845 Tanzania. J. Am. Killifsh Ass. 40(5&6):129–145.

846 Watters BR, Nagy B, van der Merwe PDW, Cotterill FPD, Bellstedt DU (2020) Redescription of
847 the seasonal killifish species *Nothobranchius ocellatus* and description of a related new species
848 *Nothobranchius matanduensis*, from eastern Tanzania (Teleostei: Nothobranchiidae). Ichthyol
849 Explor Freshw 30:151–178. http://doi.org/10.23788/IEF-1149

850 Wildekamp RH (1996) A world of killies. Atlas of the oviparous cyprinodontiform fishes of the
851 world (Vol. III). American Killifish Association, Mishawaka, 330 pp.

852 Wildekamp RH (2004) A world of killies – atlas of the oviparous cyprinodontiform fishes of the
853 world (Vol. 4). The American Killifish Association, Elyria, Ohio

854 Willemsen D, Cui R, Reichard M, Valenzano DR (2020) Intra-species differences in population
855 size shape life history and genome evolution. Elife 9:e55794.
856 https://doi.org/10.7554/eLife.55794

857 Yano CF, Bertollo LAC, Ezaz T, Trifonov V, Sember A, Liehr T, Cioffi MB (2017) Highly
858 conserved Z and molecularly diverged W chromosomes in the fish genus *Triportheus*
859 (Characiformes, Triportheidae). Heredity 118:276–283. https://doi.org/10.1038/ hdy.2016.83F

860 Yoshida K, Kitano J (2012) The contribution of female meiotic drive to the evolution of neo-sex
861 chromosomes. Evolution 66:3198–3208. https://doi.org/10.1111/j.1558-5646.2012.01681.x